Advanced Robotics

ISSN: (Print) (Online) Journal homepage: https://www.tandfonline.com/loi/tadr20

Hedge algebras-based admittance controller for safe natural human–robot interaction

Toan Nguyen Van , Soo-Yeong Yi & Phan Bui Khoi

ADVANCED ROBOTICS
2020, VOL. 34, NO. 24, 1546–1558
https://doi.org/10.1080/01691864.2020.1852958

FULL PAPER

Hedge algebras-based admittance controller for safe natural human–robot interaction

Toan Nguyen Van[a], Soo-Yeong Yi[a] and Phan Bui Khoi[b]

[a]Department of Electrical and Information Engineering, Seoul National University of Science and Technology, Seoul, South Korea; [b]School of Mechanical Engineering, Hanoi University of Science and Technology, Hanoi, Vietnam

ABSTRACT
In physical human–robot interaction (pHRI), the identification of inertia and damping matrices in the dynamic admittance model is still an open problem. Besides, the natural interaction is rarely considered in previous studies while it is crucial to obtain the effective cooperation. To this end, a fuzzy-based admittance controller is presented, in which the end-effector's velocity is adaptively adjusted via the external wrench and transmitted power without the identification of inertia and damping matrices. Besides, this fuzzy-based admittance controller also guarantees the natural cooperation between human and robot. Unfortunately, there is no formulated linkage of the fuzzy sets with the natural linguistic term semantics. As a consequence, human experts must utilize the order relationships between the terms of interest when formulating the fuzzy rule-based knowledge of the fuzzy controller. This paper presents an alternative admittance controller for pHRI based on an algebraic approach to linguistic hedges in fuzzy logic to overcome the existing shortcomings of previous admittance controllers. In addition, this paper also considers end-effector's full degree of freedom to guarantee the natural human–robot interaction. The proposed admittance controller is experimentally evaluated on a teaching task set-up using 6-DOF manipulator.

ARTICLE HISTORY
Received 27 December 2019
Revised 7 June 2020 and 16 September 2020
Accepted 12 November 2020

KEYWORDS
Hedge algebras; natural linguistic semantics; physical human–robot interaction; admittance control; fuzzy control

Nomenclature

TCP	tool center point
$\lvert\mathbf{u}\rvert$	Euclidean norm of vector $\mathbf{u}$
$<\mathbf{u},\mathbf{v}>$	Dot product of vectors $\mathbf{u}$ and $\mathbf{v}$

1. Introduction

Due to the huge interest in safe human–robot interaction, the ISO-10218 safety standard was proposed in 2011 by the International Organization for Standardization to define the safety requirements for an industrial robot [1]. As pioneers, Benjamin Navarro et al. presented an ISO10218-compliant adaptive damping controller for safe physical human–robot interaction (pHRI) in [2]. However, after all the efforts to overcome the safety issues in pHRI, the identification of inertia and damping matrices is still an open problem as this work is usually time consuming and cannot be obtained analytically. Besides, the natural cooperation between humans and robots is rarely of concern yet it is crucial to obtain the effective cooperation. In other words, the full DOF of cooperation is not considered to help operators feel naturally during the cooperation and to implement complicated tasks requiring the change of angular velocity of end-effector such as a teaching manipulator to grasp objects or to follow the welding path. These problems also exist in previous studies, for example [2–7].

By virtue of the human-like inference mechanism, fuzzy logic has been researched and applied successfully to many engineering problems [8–17]. This observation encourages Toan et al. who presented admittance controllers for safe human–robot interaction based on the inference mechanism of fuzzy logic [18,19]. In those studies, the end-effector's velocity is adaptively adjusted by an applied force (measured by a sensor mounted on the end-effector) and power transmitted by the robot without the identification of inertia and damping. Besides, the safety issue based on ISO10218 standard and natural human–robot interaction is also guaranteed [19]. Unfortunately, fuzzy logic cannot adequately simulate human language in nature since there is no formalized linkage of fuzzy sets with the natural linguistic term semantics. This drawback limits not only the ability of fuzzy sets in modeling natural language but also the performance of the designed controllers. Moreover, the fuzzy base is formulated incoherently using membership

CONTACT Phan Bui Khoi khoi.phanbui@hust.edu.vn

functions, composition of fuzzy relations, and defuzzification which may lead to errors.

By contrast, hedge algebras (HA) were proposed as an algebraic approach to the natural structure of semantic domains of linguistic variables in which linguistic values construct the semantic constraints to help linguistic terms avoid transfiguration during the handling of data. This property of HA provides experts with opportunities to discover the order relation of linguistic terms and term domains. Here, the designed fuzzy sets of terms are linked with their semantics which is interpreted as the inherent ordered-based structure. By doing this, the HA terms reflect natural linguistic properties precisely which makes the inference mechanism of the rule base to become more understandable. Furthermore, the fuzzy rule base is identified as a mathematical model using an HA-term transformation and Semantically Quantifying Mappings (SQMs). Herein, SQMs of HA are functions used to calculate the semantic values of HA terms based on the fuzziness measure. As a result, the fuzzy rule base can be defined as a real-grid-surface in Cartesian coordinates in which one fuzzy clause can be defined as a point in the Cartesian product of suitable HA. This real-grid-surface performs the semantic relationship among linguistic terms in the physical terms [20–23]. In engineering problems, this surface demonstrates the relationship among semantic values of inputs and outputs. It is clear that the semantic value of outputs can be obtained using an interpolation method on this real-grid-surface. Another difference in comparison with the inference mechanism of fuzzy logic is that the SQMs directly map the inputs' physical values to the semantic domain [0, 1]. Then, the outputs' semantic values are obtained using an interpolation method on the real-grid-surface. Therefore, to receive the physical values of outputs, their semantic values are just needed to map from [0, 1] to their physical domain. These properties give favorable conditions to apply HA to solve engineering problems in general, and control problems in particular, for example in [24–30].

This paper proposes an alternative admittance controller for safe natural human–robot interaction based on the previous works in [18,19]. The proposed controller is formulated by using HA, whose purpose is to discover the inherent ordered-based structures of the terms and term domains of linguistic variables. This approach also gives favorable conditions to reduce complexity during the controller-making-process by eliminating the membership functions, composition of fuzzy relations, and denormalization during the inference process. Instead, simple interpolation and mapping methods are used in the inference mechanism of HA. This makes the inference mechanism of the rule base to become more understandable and also reduces errors in data processing. The proposed HA-based admittance controller adaptively adjusts the end-effector's velocity using the applied wrench and power transmitted by the robot. Besides, the safety issue based on ISO10218 standard and natural human–robot interaction is also guaranteed. To our best knowledge, HA-based admittance controller is now firstly proposed for human–robot interaction.

The rest of this paper is organized as follows. In Section 2, a description of conventional admittance model and safe constraints for natural cooperation is presented. Then a fuzzy-based admittance controller for safe natural human–robot interaction is presented in Section 3. In Section 4, a brief background of HA is presented, and an admittance controller based on HA is proposed. Next, the proposed HA-based admittance controller is applied to a teaching task which uses a 6-DOF manipulator. The experiment is also implemented in several other scenarios to evaluate the performance of the proposed method in comparison to previous methods. The last section presents the conclusions of the research work.

2. Conventional admittance controller

2.1. Conventional admittance dynamic model

The admittance dynamic relationship between the end-effector's velocity and the applied forces by a human is expressed as:

$$\mathbf{B}_m(\ddot{\mathbf{x}} - \ddot{\mathbf{x}}_d) + \mathbf{D}_m(\dot{\mathbf{x}} - \dot{\mathbf{x}}_d) + \mathbf{K}_m(\mathbf{x} - \mathbf{x}_d) = \mathbf{H}, \quad (1)$$

where $\mathbf{x}$ and $\dot{\mathbf{x}} = [\mathbf{v}^T\ \mathbf{w}^T]$ are the actual tool center point (TCP) pose and velocity, $\mathbf{x}_\mathrm{d}$ and $\dot{\mathbf{x}}_d$ $\dot{\mathrm{x}}_\mathrm{d}$ are the desired TCP pose and velocity, respectively, $\mathbf{B}_\mathrm{m}$ is the desired inertia, $\mathbf{D}_\mathrm{m}$ is the desired damping and $\mathbf{K}_\mathrm{m}$ is the desired stiffness. The external wrench $\mathbf{H} = [\mathbf{F}^T\ \mathbf{M}^T]$ is the input to the admittance controller, which is external force and torque applied by human. In other words, the human is a part of the controller and it is exceedingly difficult to model the dynamics exactly. To measure the human efforts, a real-time force/torque sensor is mounted on the end-effector of the manipulator. However, it is mandatory to subtract the external forces/torques which are non-human efforts, such as gravity and inertia of the tool. For this issue, the gravity and the inertia force of the tool are calculated in its frame based on its weight and the center of mass. Then, the gravity and the inertia force of the tool are transformed to base frame of the manipulator by using transformation matrices. Similarly, the external forces/torques applied by human are also expressed in the base frame. By doing this, the actual external force/torque affected by human and the gravity and inertia force of tool are distinguished. As a result, the movement of the manipulator just depends on human efforts.

$\mathbf{K}_m$ is set to zero as no restoring force is desired, hence:

$$\mathbf{B}_m\ddot{\mathbf{x}}_{ad} + \mathbf{D}_m\dot{\mathbf{x}}_{ad} = \mathbf{H}, \tag{2}$$

where $\dot{\mathbf{x}}_{ad} = (\dot{\mathbf{x}} - \dot{\mathbf{x}}_d)$, and it is affected by the external wrench.

The virtual inertia has a negligible effect on cooperation although it is suggested that it should be adjusted proportionally to the damping for stability issues. Normally, the inertia and damping gains are pre-tuned by an operator, depending on the damping effect in each direction individually. Therefore, it is difficult to consider the requirements of safety in every DOF in the interactive space to guarantee the natural pHRI. Furthermore, it is time consuming to identify a suitable damping matrix in (2). This observation raises the need to calculate directly the end-effector's velocity, without identifying the inertia matrix and damping matrix.

2.2. Safety and natural cooperation analysis

As a crucial issue in pHRI, safety must be considered carefully to avoid unexpected accidents between robots and operators when sharing the work place. In this study, the requirements of the ISO10218 standard are qualified to cover the safety issue. To guarantee the ISO10218 standard [1,2], the force and torque must be expressed in the base frame; they are also used to calculate the power transmitted by the robot. The transformation matrix from the TCP frame to the base frame is expressed as:

$${}^{B}\mathbf{T}_T = \begin{bmatrix} {}^{B}\mathbf{R}_T & \mathbf{0}_3 \\ \mathbf{0}_3 & {}^{B}\mathbf{R}_T \end{bmatrix}, \tag{3}$$

where ${}^{B}\mathbf{R}_T$ is the rotation matrix between the TCP frame and the base frame.

The requirements are defined in ISO10218 standard as follow:

$$|\mathbf{F}| = \sqrt{F_x^2 + F_y^2 + F_z^2} \le F_{\mathrm{M}}, \tag{4}$$

$$|\mathbf{V}| = \sqrt{V_x^2 + V_y^2 + V_z^2} \le V_{\mathrm{M}}, \tag{5}$$

$$\begin{aligned} P = \langle {}^{B}\mathbf{T}_T\mathbf{H}, \dot{\mathbf{x}}\rangle &= {}^{B}F_x V_x^A + {}^{B}F_y V_y^A + {}^{B}F_z V_z^A \\ &\quad + {}^{B}M_x W_x^A + {}^{B}M_y W_y^A + {}^{B}M_z W_z^A \le P_{\mathrm{M}}, \end{aligned} \tag{6}$$

where F_{M}, V_{M}, and P_{M} are the maximum external force allowed, the maximum linear velocity allowed, and the maximum transmitted power allowed, respectively. V_x^A, V_y^A, V_z^A, W_x^A, W_y^A, and W_z^A are the measured velocity.

To guarantee safe cooperation, the dynamical relationship in (2) has to avoid inferring the constraints of the ISO10218 standard. Although the ISO10218 standard focuses uniquely on the translation components of external force $\mathbf{F}$ and linear velocity $\mathbf{V}$, the rotation components of external torque $\mathbf{M}$ and angular velocity $\mathbf{W}$ should be considered to generate natural cooperation [19]. Their effect must be suitable with the effect of translation components to get smooth cooperation, then the rotation will be determined based on $|\mathbf{V}|$ and $|\mathbf{M}|$. To do this, we also need the condition:

$$|\mathbf{M}| = \sqrt{M_x^2 + M_y^2 + M_z^2} \le M_{\mathrm{M}}, \tag{7}$$

$$|\mathbf{W}| = \sqrt{W_x^2 + W_y^2 + W_z^2} \le W_{\mathrm{M}}, \tag{8}$$

where M_{M} and W_{M} are the maximum external torque allowed and the maximum angular velocity allowed. M_{M} and W_{M} are chosen based on V_{M} and F_{M} as:

$$M_{\mathrm{M}} = F_{\mathrm{M}} L, \tag{9}$$

$$W_{\mathrm{M}} = \frac{V_{\mathrm{M}}}{L}, \tag{10}$$

with L is the the length of tool in TCP frame.

3. Fuzzy-based admittance controller

Similar to the method in [18,19], the output of the fuzzy-admittance controller is the velocity of the end-effector including linear velocity $\mathbf{V}$ and angular velocity $\mathbf{W}$. The inputs are the external wrench (including external force $\mathbf{F}$ and external torque $\mathbf{M}$) and the power transmitted by the robot P. However, in the core of the fuzzy-admittance controller, $|\mathbf{F}|$, $|\mathbf{M}|$, $|\mathbf{V}|$, $|\mathbf{W}|$, and P are used during data processing as the constraints (4)–(8) of the safety standard are used to determine the physical domain, demonstrating linguistic variables.

The fuzzy relation between inputs and the output is chosen so that the gradient of velocity changes gradually even though the external wrench changes suddenly. Based on [31], the five triangular type membership function is used for fuzzification of $|\mathbf{F}|$, $|\mathbf{M}|$, $|\mathbf{V}|$, $|\mathbf{W}|$, and P, as presented in Table 1 and Figure 1. In Figure 1, FL_i is the fuzzy set of each linguistic variable which is determined by base set X_i. *Min* and *Max* are the minimum and maximum values allowed for $|\mathbf{F}|$, $|\mathbf{M}|$, $|\mathbf{V}|$, $|\mathbf{W}|$, or P, respectively. Here, *Max* is F_{M}, V_{M}, M_{M}, or W_{M} which are identified as in the constraints (4)–(10) for inputs and outputs, respectively. *Min* is zero for all inputs and outputs as the Euclidean norm of the vector is used for safety constraints. These values are chosen based on the safety requirements of specific situations. When the values of Max are large, manipulator reacts faster in its cooperation with the human.

Table 1. Linguistic values used for fuzzification.

Z	PS	PM	P	PB
Zero	Small positive	Medium positive	Positive	Big positive

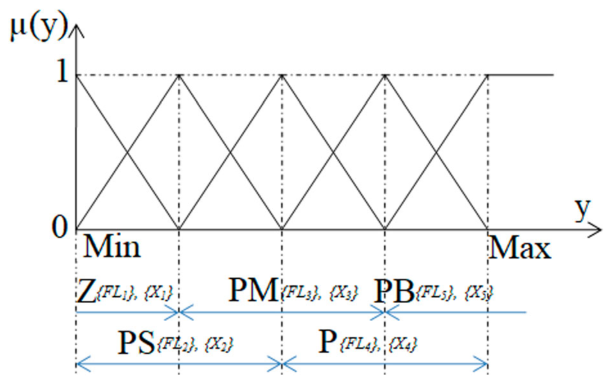

Figure 1. Five triangular type membership function for fuzzification.

Table 2. Fuzzy rule base, with inputs are |**F**| and *P*, output is |**V**|.

	|**F**|					
|**V**|	*P*	Z	PS	PM	P	PB
Z		Z	PS	PS	PM	PM
PS		PS	PS	PM	PM	P
PM		PS	PM	PM	P	P
P		PM	PM	P	P	PB
PB		PM	*P*	P	PB	PB

To guarantee natural cooperation, both translation and rotation components should be considered. However, it is important to understand that errors in rotation are much more significant than errors in translations. Therefore, translation components should be calculated first. Then, rotation components should be considered in relationship with the translation components so that it guarantees smooth cooperation. Here, the value of |**V**| is calculated through |**F**| and the power transmitted by the robot, *P*, using the fuzzy rule base in Table 2. Then, the value of |**W**| is calculated via |**V**| and |**M**|. The relationship between |**V**|, |**M**|, and |**W**| is presented in Table 3, and the objective is to generate smooth cooperation (|**W**| does not change too fast, but it has to respond to the external torque timely). Using the relationship between the end-effector's velocity and external wrench and power transmitted by the robot as presented in Tables 2 and 3, the identification of the damping matrix is avoided.

To infer the fuzziness of outputs, a composition operator must be used to measure the fuzziness of every fuzzy clauses in the fuzzy rule base first. Then, they are integrated to obtain the final fuzziness of the output. In this paper, the max–min composition is used. This composition is defined by (11) and (12) as follows:

Table 3. Fuzzy rule base, with inputs are |**M**| and |**V**|, output is |**W**|.

	|M|					
|W|	|V|	Z	PS	PM	P	PB
Z		Z	Z	PS	PS	PM
PS		Z	PS	PS	PM	PM
PM		PS	PS	PM	PM	P
P		PS	PM	PM	P	P
PB		PM	PM	P	P	PB

$$\mu(\mu_A, \mu_B) = min(\mu_A, \mu_B), \tag{11}$$

$$\mu_{A\cup B}(x) = \max\{\mu_A(x), \mu_B(x)\}, \tag{12}$$

As the obtained values after implementing the composition of fuzzy relations are the fuzziness of outputs, a defuzzification is inevitable to map the fuzziness values to the desired physical values. Based on [32], the centroid defuzzification is chosen. In this approach, the physical value is identified by the horizontal degree of center of the region which is created by the horizontal axis and the membership function $\mu_{B'}(x)$, shown as

$$x' = \frac{\int_S x\mu_{B'}(x)dx}{\int_S \mu_{B'}(x)dx}, \tag{13}$$

As mentioned in Section 1, the fuzzy approach consists of some shortcomings, which relate to the inference mechanism of the fuzzy logic. This analysis raises the need to use an alternative approach to improve the performance of the admittance controller.

4. HA-Based admittance controller

4.1. *Background on HAs*

HAs were developed to discover the inherent order-based structures of terms and term domains of linguistic variables which helps the semantic relationship of terms and term domains approach to the inference mechanism in nature. From this viewpoint, every term-domain of a linguistic variable X can be considered as an HA,$AX = (\mathbf{X}, \mathbf{G}, \mathbf{C}, \mathbf{H}, \leq)$ [20–24].

- $(\mathbf{X}, \leq)$ is an order-based structure, where $\mathbf{X} \subseteq Dom(X)$ is a term-set of a linguistic variable X; and $\leq$ is an order relation on **X.**
- $\mathbf{G} = c^-, c^+$ is a set of generators, where c^- is the negative primary term and c^+ is the positive primary term, with $c^- \leq$ c+.

- $\mathbf{C} = \mathbf{0}, W, \mathbf{1}$ is the set of fixed points, satisfying $\mathbf{0} \leq c^- \leq W \leq c^+ \leq \mathbf{1}$, where $\mathbf{0}$, $\mathbf{1}$ and W stand for the least, the greatest, and the neutral term in the structure $(\mathbf{X}, \leq)$, respectively.
- $\mathbf{H_I} = \mathbf{H} \cup \mathbf{I}$, where $\mathbf{H} = \{\mathbf{H}^-, \mathbf{H}^+\}$ is a set of unary operations representing linguistic hedges of $\mathbf{X}$ in which $\mathbf{H}^- = \{h_j : -q \leq j \leq -1\}$ and $\mathbf{H}^+ = \{h_j : 1 \leq j \leq p\}$ stand for the set of *negative* and *positive* hedges, respectively; where q is the number of negative hedges and p is the number of positive hedges. If the hedges are characterized by $h \in \mathbf{H}$, we have:
  - $hc^+ \leq c^+$, and $hc^- \geq c^-$ if $h \in \mathbf{H}^-$
  - $hc^+ \geq c^+$, and $hc^- \leq c^-$ if $h \in \mathbf{H}^+$

I, regarded as an artificial hedge, is the identity of X, hence $\mathbf{I}x = x, \forall x \in X$. This definition is presented to simplify and/or unify the formulation of certain formulas and statements [23]. By doing this, $x \in \mathbf{H}_\mathrm{I}(x)$ is always valid, where $\mathbf{H}_\mathrm{I}(x)$ is the set of all terms of AX, generated from x using hedges in $\mathbf{H}_\mathrm{I}$. In the case of $x = h_m, \ldots, h_j \mathbf{I} h_{j-1}, \ldots, h_1 c$, where $c \in \mathbf{G} \cup \mathbf{C}$ and h_j $\in \mathbf{H}$ with $j = 1, \ldots, m$, the hedges $h_m, \ldots, h_j$ have no effect on $\mathrm{I}h_{j-1}, \ldots, h_1\mathrm{c}$. Therefore,

$$x = h_m, \ldots, h_j \mathbf{I} h_{j-1}, \ldots, h_1 c = h_{j-1}, \ldots, h_1 c, \tag{14}$$

Besides, the order relation of all terms in $\mathbf{H}_\mathrm{I}(x)$ can be performed:

- If $h \neq k$ $(h, k \in \mathbf{H_I})$, and $hx \leq kx$, then $h'hx \leq k'kx$, $\forall h', k' \in \mathbf{H_I}$
- If $h \in \mathbf{H_I}$, $hx \leq x$, then $h'hx \leq x$, $\forall h' \in \mathbf{H_I}$
- If $hx = x$, then x is a fixed point
- If $x \notin H_I(y)$ and $y \notin H_I(x)$, then x and y are independent.

By virtue of $\mathbf{H}_\mathrm{I}$ and $\mathbf{G} \cup \mathbf{C}$, the terms are generated as

$$\mathbf{X} = \mathbf{H}_I(\mathbf{C} \cup \mathbf{G}) = \mathbf{C} \cup \mathbf{H}_I(c^-) \cup \mathbf{H}_I(c^+), \tag{15}$$

$$\{\mathbf{0}\} \leq \mathbf{H}_I(c^-) \leq \{W\} \leq \mathbf{H}_I(c^+) \leq \{\mathbf{1}\}, \tag{16}$$

The semantic structure of AX is based on definitions of the fuzziness measure and SQMs.

4.1.1. Fuzziness measure

The fuzziness values of an element τ always belong to [0, 1] $\forall \tau \in X$, which is calculated by a given fuzziness measure, denoted as $f_m(\tau)$ [20]. It is clear that $f_m(\tau) = 0$ if τ is clear i.e., $f_m(\mathbf{0}) = f_m(\mathbf{W}) = f_m(\mathbf{1}) = 0$. Several specific properties of fuzziness measure can be performed as shown in (17)–(22), where h is a hedge and τ is a fuzzy value.

$$\frac{f_m(hx)}{f_m(x)} = \frac{f_m(hy)}{f_m(y)}, \ \forall x, y \in X, \ h \in \mathbf{H}_I, \tag{17}$$

$$f_m(h\tau) < f_m(\tau), \forall \tau \in \mathbf{X}, \tag{18}$$

$$f_m(h\tau) = \mu(h) f_m(\tau), \forall \tau \in X, \tag{19}$$

where $\mu(h)$ are commonly called the fuzziness parameters of $\mathbf{X}$.

If c^+ and c– are two primary terms in $\mathbf{X}$, then

$$f_m(c^+) + f_m(c^-) = 1, \tag{20}$$

$$\sum\nolimits_{h \in H} f_m(h\tau) = f_m(\tau), \ \forall \tau \in \mathbf{X}, \tag{21}$$

Recursively, for $x = h_\mathrm{m}, \ldots, h_1 c \in \mathbf{X}$, where $c \in \mathbf{G}$,

$$\sum_{h \in H} \mu(h) = 1 \text{ and } f_m(x) = \mu(h_m) f_m(x|_m)$$
$$= \mu(h_m) \ldots \mu(h_1) f_m(c), \tag{22}$$

where $x|_m = h_{m-1}, \ldots, h_1 c$ is the m^{th} – suffix of x.

4.1.2. SQMs

Using f_m as a fuzziness measure function of $\mathbf{X}$, semantically quantifying mapping $\upsilon: \mathbf{X} \rightarrow [0, 1]$, combining with f_m, is determined as [21]:

$$\upsilon(\mathbf{W}) = \theta = f_m(c^-), \tag{23}$$

$$\upsilon(c^-) = \theta - \alpha f_m(c^-) = \beta f_m(c^-), \tag{24}$$

$$\upsilon(c^+) = \theta + \alpha f_m(c^+), \tag{25}$$

$$\upsilon(h_j x) = \upsilon(x) + Sgn(h_j x) \left\{ \sum_{i=Sgn(j)}^{j} f_m(h_i x) - \omega(h_j x) f_m(h_j x) \right\}, \tag{26}$$

where

$$\omega(h_j x) = \frac{1}{2}[1 + Sgn(h_j x) Sgn(h_p h_{j-1} x)(\beta - \alpha)], \tag{27}$$

$$j \in \{-q \leq j \leq p, j \neq 0\} = [-q \ldots p] \tag{28}$$

$$\sum_{i=-q}^{-1} \mu(h_i) = \alpha$$

and

$$\sum_{i=1}^{p} \mu(h_i) = \beta$$

with $\alpha, \beta > 0$ and $\alpha + \beta = 1$.

Sgn is the sign function of hedges and terms. $sgn(c^+) = +1$ and $sgn(c^-) = -1$ as c^+ and c^- possess the positive tendency and negative tendency, respectively. Based on the effect of hedges on the terms of X, $sgn(h) = +1$ if h $\in \mathbf{H}^+$ and $sgn(h) = -1$ if h $\in \mathbf{H}^-$. In addition, given the action effect of hedges, one hedge may have a relative sign with respect to another: $sgn(h,k) = +1$ or, $sgn(h,k) = -1$, depending on whether h strengthens or weakens the effect tendency of k. Now, for a point which is not fixed, also has a sign defined by:

$$sgn(x) = sgn(h_m, h_{m-1}) \dots sgn(h_2, h_1) sgn(h_1) sgn(c) \quad \forall \mathrm{x} = \mathrm{h}_m \dots h_1 c, \tag{29}$$

The meaning of the sgn function is that:

- If $sgn(hx) = +1$, then $hx \geq x$
- If $sgn(hx) = -1$, then $hx \leq x$

4.2. HA-based admittance controller

To construct HA controllers that solve the mentioned engineering problems in existing admittance controllers, the following scheme which includes three main tasks should be conducted:

- Identification of HA-terms: the ordinary linguistic labels of the fuzzy rule base are converted into HA-terms; whose purpose is to perform the linguistic variables in the order relation.
- Quantifying the rule base: the rule base is converted into a real surface in the Euclidean space using SQMs. This surface demonstrates the relationship between the semantic values of inputs and outputs.
- Control algorithm and denormalization: a control algorithm is formulated to solve the given control problem and adjusting the term semantics. Then, the semantics of outputs are denormalized to physical values based on a mapping method.

As an inheritance of the fuzzy-admittance controller and the described HA scheme, an HA-based admittance controller is formulated to solve the existing problems and improve the performance of the admittance controller.

First, to determine the linguistic rule base for the HA-based admittance controller, the HA for all linguistic variables of $|\mathbf{F}|$, $|\mathbf{M}|$, $|\mathbf{V}|$ and $|\mathbf{W}|$ must be identified to constitute a suitable transformation of linguistic labels into the respective HA terms. In general, the HA of linguistic variables can be facultative. However, they are assumed to be similar in this paper to perform their relationship in a unified form. Then, the similar sets $\mathbf{G}$, $\mathbf{C}$, and $\mathbf{H_I}$ for all HA are chosen as follows:

- $\mathbf{G} = \{\mathrm{S}, \mathrm{B}\}$, where $c^- = \mathrm{S}$, and $c^+ = \mathrm{B}$. S and B stand for Small and Big, respectively.
- $\mathbf{C} = \{\mathbf{0}, W, \mathbf{1}\}$, where $\mathbf{0}$, W, and $\mathbf{1}$ are fixed points, known respectively as the least, the medium, and the greatest terms of the determined HA.
- $\mathbf{H}_\mathrm{I} = \{\mathrm{L}, \mathrm{V}\} \cup \{\mathbf{I}\}$, where $\boldsymbol{h}^- = \mathrm{L}$; $\boldsymbol{h}^+ = \mathrm{V}$, with L and V stand for Little and Very, respectively.

Given the defined sets, the linguistic hedges S and V of $\mathbf{G}$ combine with generators L and V of $\mathbf{H}$ to create whole term-set $\mathbf{X}$ of every HA of linguistic variables in the linearly ordered relation, $\mathbf{X} = \{\mathbf{0}, \mathrm{VS}, \mathrm{LS}, \boldsymbol{W}, \mathrm{LB}, \mathrm{VB}, \mathbf{1}\}$. Then, the fuzzy-terms of $|\mathbf{F}|$, $|\mathbf{M}|$, $|\mathbf{V}|$, and $|\mathbf{W}|$ are converted into HA-terms based on a term transformation as presented in Table 4. Here, the term-transformations should reserve the order relations and opposite meaning of terms. It is noticed that the term-set $\mathbf{X}$ in every HA of $|\mathbf{F}|$, $|\mathbf{M}|$, $|\mathbf{V}|$, and $|\mathbf{W}|$ is defined similarly, which means that the semantic relationship and semantic values of HA terms of the linguistic variables may be similar. However, the semantic values of HA terms of $|\mathbf{F}|$, $|\mathbf{M}|$, $|\mathbf{V}|$, and $|\mathbf{W}|$ just perform their semantic relationship individually as their physical domains are different. Therefore, by mapping their semantic values to their real physical domain, we observe different values for different inputs and outputs. This is similar in the fuzzy controller where the linguistic values of inputs and outputs are similar, but their physical domains are different. Next, the fuzzy rule base for $|\mathbf{V}|$ and $|\mathbf{W}|$ in Tables 2 and 3 are transformed into the HA rule base as presented in Tables 4–6. As mentioned earlier, the semantics of HA terms belong to the domain [0, 1], and therefore, the points $\mathbf{0}$ and $\mathbf{1}$ are used in the HA rule base as semantic bound for interpolation methods and to avoid the loss of the data during processing.

Table 4. Term transformation of the linguistic values.

For FL	–	Z	PS	PM	P	PB	–
For HA	**0**	VS	LS	**W**	LB	VB	**1**

Table 5. HA rule base, with inputs are $|\mathbf{F}|$ and P, output is $|\mathbf{V}|$.

$\lvert\mathbf{V}\rvert$	$\lvert\mathbf{F}\rvert$ / P	***0***	VS	LS	***W***	LB	VB	***1***
	0	0	VS	VS	LS	LS	W	W
	VS	VS	VS	LS	LS	W	W	LB
	LS	VS	LS	LS	W	W	LB	LB
	W	LS	LS	W	W	LB	LB	VB
	LB	LS	W	W	LB	LB	VB	VB
	VB	W	W	LB	LB	VB	VB	1
	1	W	LB	LB	VB	VB	1	1

Table 6. HA rule base, with inputs are |**M**| and |**V**|, output is |**W**|.

	|M|							
|W|	|V|	*0*	VS	LS	*W*	LB	VB	*1*
0		*0*	*0*	VS	VS	LS	LS	W
VS		*0*	VS	VS	LS	LS	W	W
LS		VS	VS	LS	LS	W	W	LB
W		VS	LS	LS	W	W	LB	LB
LB		LS	LS	W	W	LB	LB	VB
VB		LS	W	W	LB	LB	VB	VB
1		W	W	LB	LB	VB	VB	*1*

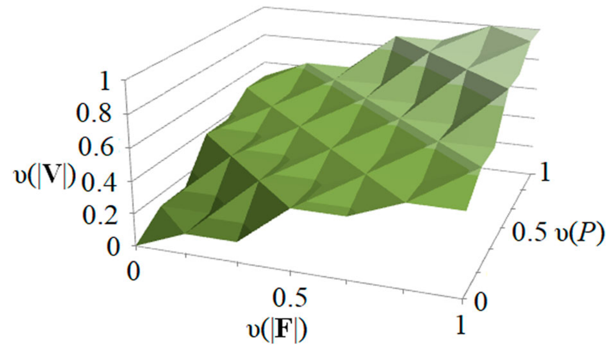

Figure 2. The real-grid-surface describes the semantic relationship between |**V**|, |**F**| and *P*.

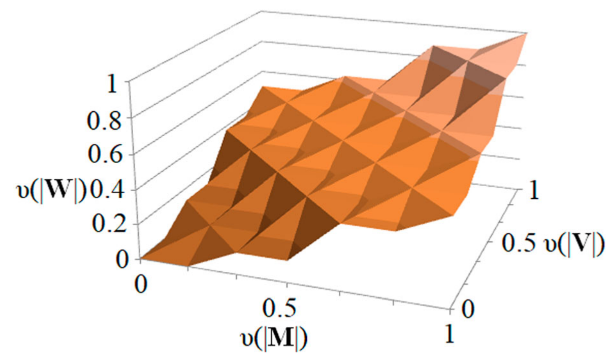

Figure 3. The real-grid-surface describes the semantic relationship between |**W**|, |**M**| and |**V**|.

As **G** uniquely consists of two primary terms S and B, and the effect of S and B on L and V of **H** to create HA terms are similar, the fuzziness of the primary terms and hedges are measured through (17) to (22) as:

$$f_m(\mathrm{S}) = \theta = 0.5; \mu(\mathrm{L}) = \mu(\mathrm{V}) = 0.5 \rightarrow \alpha$$
$$= \beta = 0.5 \text{ and } f_m(\mathrm{B}) = 1 - f_m(\mathrm{S}) = 0.5.$$

Besides, **H** just includes two linguistic hedges, and therefore we have $q = 1$, and $p = 1$.

Now, the SQM is used to calculate the semantics of HA terms, whose purpose is to identify the mathematical model of the HA rule base. Based on Tables 5 and 6, and (23) to (29), the HA rule base of |**V**| and |**W**| in Tables 5 and 6 is transformed into the semantic relationships as presented in Tables 7 and 8. The semantic relationship between |**F**|, *P*, and |**V**| in Table 7 defines the super surface in Euclidean space as shown in Figure 2. The semantic relationship between |**M**|, |**V**|, and |**W**| in Table 8 defines the super surface in the Euclidean space as shown in Figure 3.

Finally, an interpolation is used to approximate the semantic values of |**V**| and of |**W**| through the semantic relationships among inputs and outputs in Tables 7 and 8. Normally, the product operator and the average operator are used to approximate the semantic values

Table 7. The semantic relationship of |**F**|, *P* and |**V**|.

		|F|						
|V|		$\upsilon(0) = 0$	$\upsilon(\mathrm{VS}) = 0.125$	$\upsilon(\mathrm{LS}) = 0.375$	$\upsilon(W) = 0.5$	$\upsilon(\mathrm{LB}) = 0.625$	$\upsilon(\mathrm{VB}) = 0.875$	$\upsilon(1) = 1$
P	$\upsilon(0) = 0$	0	0.125	0.125	0.375	0.375	0.5	0.5
	$\upsilon(\mathrm{VS}) = 0.125$	0.125	0.125	0.375	0.375	0.5	0.5	0.625
	$\upsilon(\mathrm{LS}) = 0.375$	0.125	0.375	0.375	0.5	0.5	0.625	0.625
	$\upsilon(W) = 0.5$	0.375	0.375	0.5	0.5	0.625	0.625	0.875
	$\upsilon(\mathrm{LB}) = 0.625$	0.375	0.5	0.5	0.625	0.625	0.875	0.875
	$\upsilon(\mathrm{VB}) = 0.875$	0.5	0.5	0.625	0.625	0.875	0.875	1
	$\upsilon(1) = 1$	0.5	0.625	0.625	0.875	0.875	1	1

Table 8. The semantic relationship of |**M**|, |**V**| and |**W**|.

		|M|						
|W|		$\upsilon(0) = 0$	$\upsilon(\mathrm{VS}) = 0.125$	$\upsilon(\mathrm{LS}) = 0.375$	$\upsilon(W) = 0.5$	$\upsilon(\mathrm{LB}) = 0.625$	$\upsilon(\mathrm{VB}) = 0.875$	$\upsilon(1) = 1$
|V|	$\upsilon(0) = 0$	0	0	0.125	0.125	0.375	0.375	0.5
	$\upsilon(\mathrm{VS}) = 0.125$	0	0.125	0.125	0.375	0.375	0.5	0.5
	$\upsilon(\mathrm{LS}) = 0.375$	0.125	0.125	0.375	0.375	0.5	0.5	0.625
	$\upsilon(W) = 0.5$	0.125	0.375	0.375	0.5	0.5	0.625	0.625
	$\upsilon(\mathrm{LB}) = 0.625$	0.375	0.375	0.5	0.5	0.625	0.625	0.875
	$\upsilon(\mathrm{VB}) = 0.875$	0.375	0.5	0.5	0.625	0.625	0.875	0.875
	$\upsilon(1) = 1$	0.5	0.5	0.625	0.625	0.875	0.875	1

of outputs. However, these operators easily cause loss of data as they transform the super surface to a 2-D curve before interpolation. This observation raises the need to use the four-point bi-linear interpolation [33] as this method directly uses the 3-D super surface, especially this real-grid-surface is square grid. By doing this, the risk of errors is reduced, the software implementation is simplified, and the interpolation mechanism is easier to understand. Until now, only the semantic values of outputs $|\mathbf{V}|$ and $|\mathbf{W}|$ are known. To receive their real physical values, their term semantics is mapped from $[0, 1]$ to their individual physical domains.

4.3. End-effector's velocity

Instead of directly using the values of $|\mathbf{V}|$ and $|\mathbf{W}|$, six components of velocity are determined. As the value of each element of the external wrench directly affects the value of each element of velocity, we use $|\mathbf{V}|$ and $|\mathbf{F}|$ to calculate the velocity's translation components, and $|\mathbf{W}|$ and $|\mathbf{M}|$ to calculate the velocity's rotation. The velocity's elements of end-effector can be calculated by (30)–(31):

$$V_j = \begin{bmatrix} \frac{F_j|\mathbf{V}|}{|\mathbf{F}|} & if\,|\mathbf{F}| \neq 0 \\ 0 & if\,|\mathbf{F}| = 0 \end{bmatrix}, \tag{30}$$

$$W_j = \begin{bmatrix} \frac{M_j|\mathbf{W}|}{|\mathbf{M}|} & if\,|\mathbf{M}| \neq 0 \\ 0 & if\,|\mathbf{M}| = 0 \end{bmatrix}, \tag{31}$$

where j indicates the direction of x, y or z axis.

4.4. Stability considerations

In pHRI, the human uses haptic and visual feedback from the plant to regulate their actions. Therefore, the human is part of the controller and it is exceedingly difficult to model and prove the overall stability of the system. In previous admittance controllers, the imposition of the dynamic admittance model is the relationship between the external force and the end-effector's velocity. In other words, the linear velocity of the end-effector only depends on the translation elements of the external wrench, and the angular velocity of the end-effector only depends on the rotation elements of external wrench. As a consequence, it can lead to a large jerk during the cooperation if the external wrench changes sharply. Experimental studies on the impedance control [34] showed that the robot could present unstable behavior with very low virtual damping and high virtual inertia of stiff environment. It is suggested that the human arm has a maximum impedance [35] that occurs when the human increases the stiffness of their arm. Normally, to prevent the instability of the human–robot system for conventional admittance controller, the virtual inertia during the cooperation is constant and equal to half the effective inertia of the manipulator in the direction of the motions. The effective mass $\mathbf{B}_t$ is expressed as:

$$\mathbf{B}_t^{-1}(\mathbf{q}) = \mathbf{J}(\mathbf{q})\mathbf{M}^{-1}(\mathbf{q})\mathbf{J}^T(\mathbf{q}), \tag{32}$$

where $\mathbf{M} \in R^{6x6}$ is the mass matrix of the manipulator's configuration space, $\mathbf{B}_t \in R^{6x6}$ is the effective mass in the frame, and $\mathbf{J}$ is the Jacobian matrix.

By contrast, the stability and accuracy of fuzzy-based and HA-based controllers mainly depend on the expert knowledge-based rule base. As analyzed in [36], the fuzzy controller can be stable and ensure the accuracy by choosing a good fuzzy rule and physical value domain of appropriate input and output variables. Furthermore, the mathematical foundation given by HA seems to form a new approach to solve fuzzy control problems, which is quite different from that based on the fuzzy sets. It has been shown that the HA-based controller causes smaller errors and, moreover, it can bring the controlled object to a stable state, while the controller based on other methods cannot. This point is clearly analyzed in [37,38].

In addition, to avoid the direct map from external forces/torques to linear/angular velocities, the proposed admittance controller uses additional input which is transmitted power in comparison with previous admittance controllers. This input is a combination of external wrench and actual velocity, calculated by formula (6). In this paper, the natural human–robot interaction is also considered. It means that the velocity of end-effector and external forces include both linear and angular elements. Normally, the rotation elements have bigger effects on the stability and accuracy than translation elements since a small change of the rotation can lead to a big error. This observation raises the need to create a relationship between linear velocity and angular velocity to guarantee the smooth cooperation. Based on this point, the linear velocity is calculated first based on translation elements of external wrench and transmitted power, then angular velocity is calculated based on linear velocity and rotation elements of external wrench. As shown in formula (6), the values of transmitted power depend on $\mathbf{V}_{k-1}$, $\mathbf{W}_{k-1}$, $\mathbf{F}$, and $\mathbf{M}$. It is clearly seen that the values of transmitted power will not change sharply even when external wrench changes dramatically. Based on rule bases in Tables 2 and 5, the values of linear velocity will not change suddenly. Similarly, the values of angular velocity will also not change suddenly based on the relationship between $|\mathbf{W}|$ and $|\mathbf{M}|$ and $|\mathbf{V}|$ in Tables 3 and 6. This helps to reduce the jerk during cooperation between the human and the robot. This point also can be clearly shown in the experimental results.

5. Estimation

5.1. Set-up

The proposed HA-based admittance controller is evaluated by a teaching task set-up using a 6-DOF manipulator in which a real-time force/torque sensor is mounted at the end-effector. This set-up is shown in Figure 4 where the blocks work as elements of a distributed system. First, the client on the computer sends the desired assignments of the operator to the master controller via the TCP/IP protocol. Then, based on the received assignments from the computer and the data from the real-time force/torque sensor, the master controller processes and sends the control commands to slave controllers (the circle time $T_{com} = 1$ ms). These slave controllers are used to control motors at the joints of the robot. The CAN protocol is used for communication between the master controller and the real-time force/torque sensor, and the circle time to send and receive data is 1 ms ($T_{CAN} = 1$ ms). To guarantee the requirements of the ISO10218 standard, the maximum values allowed of |F|, |V|, and P should be given. In this paper, these values are set to $F_M = 120$ N, $V_M = 0.12$ m/s, $P_M = 15$ W, and $L = 0.058$ m (note that the tool is the part which is attached to real-time force/torque sensor and operators hold this part to cooperate with manipulator).

5.2. Control framework

The workflow of the experimental set-up is shown in Figure 5. At each iteration, the admittance controller calculates the velocity of the end-effector based on the external wrench and power transmitted by the robot. Depending on the scenario, the admittance controller can be the proposed HA-based admittance controller, fuzzy-based admittance controller or the conventional admittance controller. The desired joint velocities of the manipulator are calculated using inverse kinematics with the Jacobian method. Finally, the joints of the manipulator are controlled by PID method to follow the desired values. In this experimental set-up, the manipulator passively moves based on human effort.

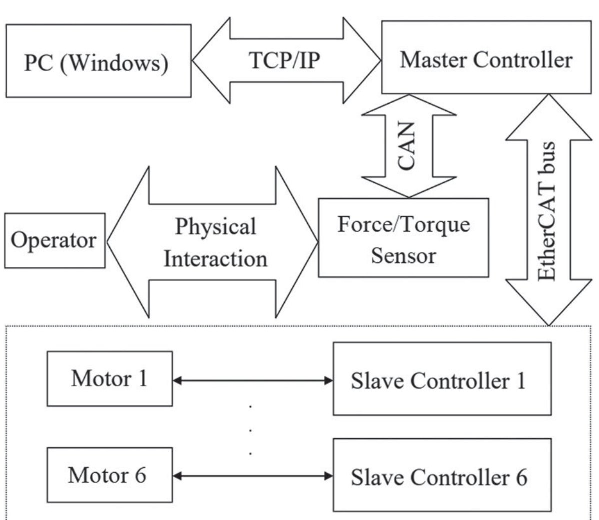

Figure 4. The system interface for human–robot interaction.

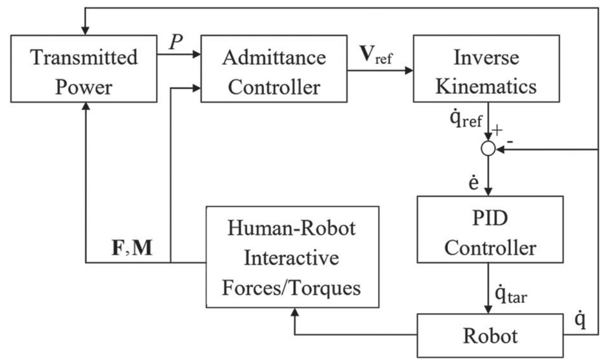

Figure 5. Workflow of human–robot interaction system.

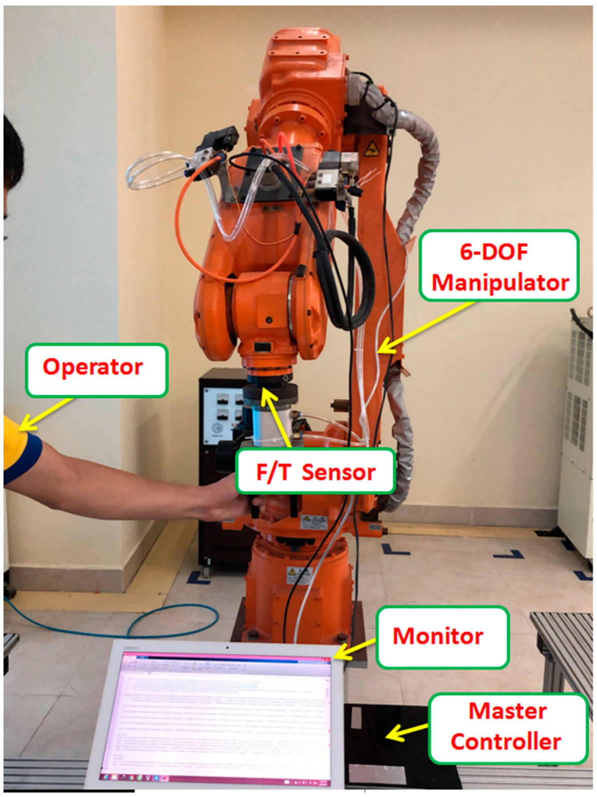

Figure 6. Experimental set-up for teaching tasks, the operator pushes and pulls the end-effector to some desired positions. The manipulator then memorizes these desired positions for later work. This can be applied to set the positions for object pick-up tasks.

5.3. Implementation

The experiments of the teaching task for the manipulator are conducted as shown in Figure 6 where the operator pushes and pulls the end-effector to some desired positions. The manipulator then memorizes these desired positions for later work. This can be applied to set the positions for object pick-up tasks.

In this study, the teaching task consists of three stages: first, the end-effector moves to the position of an object (I), then the end-effector moves to the desired target position (II); and finally, the end-effector moves back to the initial position (III).

As mentioned before, this experiment is conducted for several different scenarios using the proposed HA-based admittance controller, fuzzy-admittance controller and the conventional admittance controller. Their comparison verifies the performance of the proposed controller.

Table 9. Estimated errors of admittance controllers.

Method			HA	FA	AD
Mean (%)		$\Delta\lvert V\rvert$	3.39	4.02	5.45
		$\Delta\lvert W\rvert$	10.88	12.45	13.68
Mean	(mm/s)	$\lvert V_{k+1} - V_k\rvert$	0.48	0.56	0.85
	(rad/s)	$\lvert W_{k+1} - W_k\rvert$	0.0076	0.0092	0.0126
|F| (N)		Max	83.42	83.18	75.70
		Mean	53.82	54.84	47.68
|M| (N m)		Max	1.58	1.58	2.11
		Mean	0.62	0.56	0.59

Notes: HA is the HA-admittance controller, FA is the fuzzy-admittance controller, AD is the conventional admittance controller. |**F**| is the norm of external force and |**M**| is the norm of external torque. The error and the step of velocity obtained from HA-based admittance controller are smallest compared to other controllers.

The manipulator reacts differently depending on the person who participates in the human–robot cooperation as the interaction is affected by human factors. This raises the need to implement experiments with a group of different persons. In this paper, the experiments are conducted by a group of 10 persons, of which 8 are men and 2 are women, and their age ranges from 23 to 55 years. Each person cooperates with the manipulator to serve a similar teaching task in three different scenarios, as discussed next.

5.4. Results

To estimate the accuracy of controllers, the percentage error in (33) is used.

$$\Delta = \left|\frac{\text{measured velocity - calculated velocity}}{\text{calculated velocity}}\right| \times 100\%, \tag{33}$$

The results are presented in Table 9, and Figures 7–10. In Table 9, HA represents the HA-admittance controller, FA is the fuzzy-admittance controller, AD is the conventional admittance controller, with experimental damping gains of 3.33, 5, 3.33, 0.33, 0.5, 0.33. The units of measurements are Ns/m and Nms/rad for translation damping gains and rotation damping gains, respectively. The horizontal red lines in Figures 7–9 are the maximum allowed values of the norm of linear velocity.

The obtained results show that the proposed HA-based and the fuzzy-based admittance controllers give favorable conditions to avoid instability during the cooperation even when the external wrench is suddenly

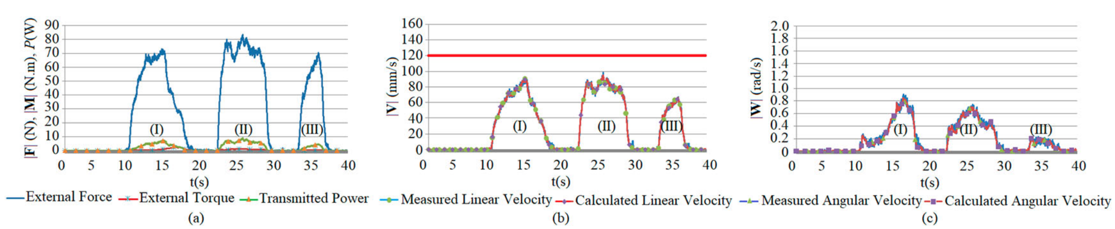

Figure 7. Experimental results obtained HA-based admittance controller, (a) external force |**F**| (N), torque magnitude |**M**| (N m) and the transmitted power *P* (W); (b) tool linear velocity |**V**| (mm/s), here the horizontal red line is the maximum allowed values of the norm of linear velocity; (c) tool angular velocity |**W**| (rad/s)

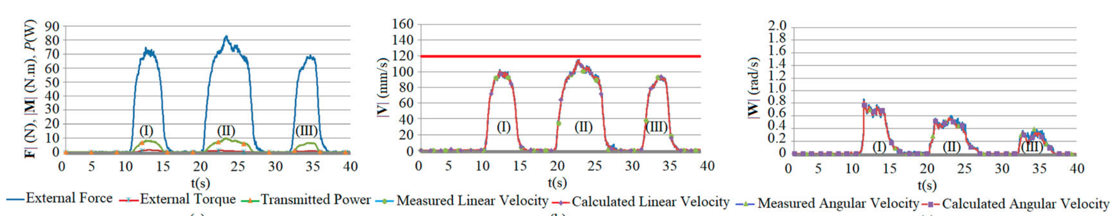

Figure 8. Experimental results obtained from fuzzy-based admittance controller, (a) external force |**F**| (N), external torque |**M**| (N m) and the transmitted power *P* (W); (b) tool linear velocity |**V**| (mm/s), here the horizontal red line is the maximum allowed values of the norm of linear velocity; (c) tool angular velocity |**W**| (rad/s)

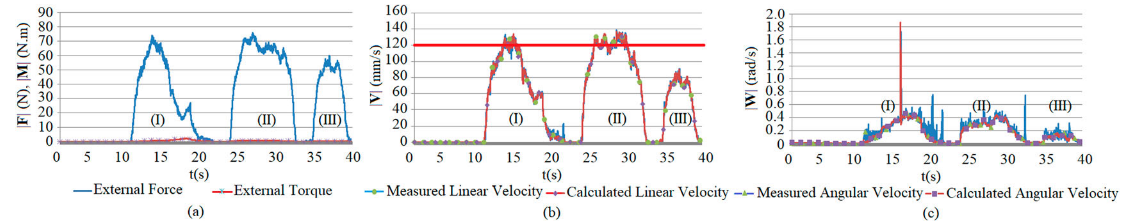

Figure 9. Experimental results obtained from conventional admittance controller (with damping gain $D = 3.33, 5, 3.33, 0.33, 0.5, 0.33$), (a) external force $|\mathbf{F}|$ (N) and external torque $|\mathbf{M}|$ (N m); (b) tool linear velocity $|\mathbf{V}|$ (mm/s), here the horizontal red line is the maximum allowed values of the norm of linear velocity; (c) tool angular velocity $|\mathbf{W}|$ (rad/s)

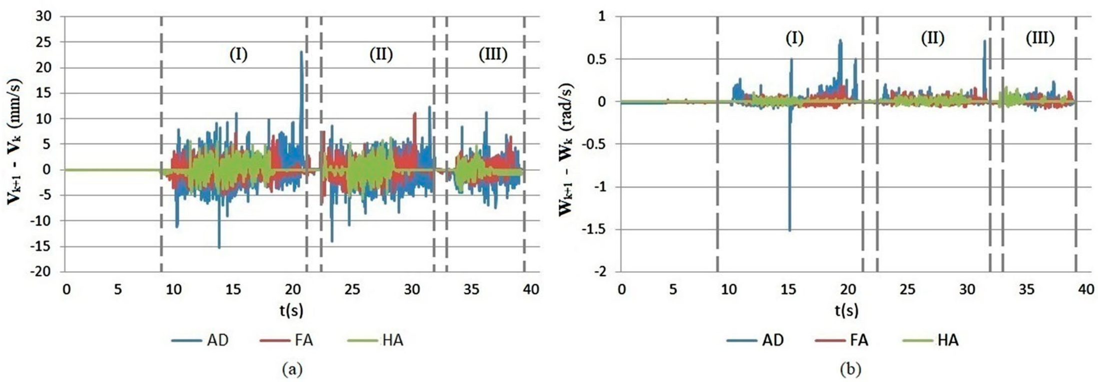

Figure 10. The variation of end-effector during teaching task, (a) the variation of linear velocity (mm/s), (b) the variation of angular velocity (rad/s). Here, AD is conventional admittance controller, FA is fuzzy-based admittance controller, and HA is hedge algebras-based admittance controller. HA-based admittance controller is found to provide better velocities compared to other controllers.

changed. This can be clearly seen in Figure 10 where obtained results from conventional admittance controller include some peaks, whereas there is no peak in the results from fuzzy-based and HA-based admittance controllers. Furthermore, based on Table 9, it is easy to see that the HA-based admittance controller is the most accurate and its inference mechanism is much easier than the inference mechanism of the fuzzy-based admittance controller as it eliminates the use of the membership functions, the composition of fuzzy relation and defuzzification. The mean of velocity step for each admittance controller is presented in Table 9; for the proposed HA-based admittance controller, the linear velocity step is 0.48 mm/s and the angular velocity step is 0.0076 rad/s whereas the linear velocity steps are 0.56 and 0.85 mm/s and angular velocity steps are 0.0092 and 0.0126 rad/s for the fuzzy-based and conventional admittance controllers, respectively. In addition, for the proposed HA-admittance controller, the percentage errors of linear velocity and angular velocity are 3.39% and 10.88%, respectively. These percentage errors increase 4.02%, 5.45%, and 12.45%, 13.68% for the fuzzy-based and conventional admittance controllers, respectively. The applied values of the external wrench in every DOF in the interactive space are always constrained based on the ISO10218 standard to guarantee safe and natural pHRI. Therefore, the velocity of the end-effector always belongs in a safe domain even when the external wrench is larger than the allowed value.

6. Conclusions

This paper proposed an admittance controller based on an algebraic approach to linguistic hedges in fuzzy logic to eliminate the identification of inertia and damping matrices. In the proposed controller, the end-effector's velocity is adjusted directly through the external force and the robot's transmitted power. Besides, natural human–robot cooperation and the safety issue based on ISO10218 standard are considered. Furthermore, this controller overcomes several limitations of the fuzzy-admittance controller, namely avoiding the use of the membership function, composition of fuzzy relations, and defuzzification in building the controller. By doing this, the inference mechanism of controller is much easier. Additionally, linguistic variables can be compared with each other using the HA approach.

Disclosure statement

No potential conflict of interest was reported by the author(s).

Funding

This research was partly supported by the research program funded by the National Research Foundation of Korea [grant number NRF-2018R1D1A1B07044841].

Notes on contributors

Nguyen Van Toan received the Degree of Engineer in Mechatronics from Center for Training of Excellent Students, Hanoi University of Science and Technology, in 2014. He studied Master course and researched at Korea Institute of Science and Technology, Seoul, South Korea until 2018. He is now studying forward to PhD program at Department of Electrical and Information Engineering, Seoul National University of Science and Technology, Seoul, South Korea. His current research interests include robotics, fuzzy control, expert knowledge, artificial intelligence, hedge algebras, and genetic algorithm.

Soo-Yeong Yi received his M.S. and Ph.D. degrees in Electrical Engineering from Korea Advanced Institute of Science and Technology, in 1990 and 1994, respectively. During 1995–1999, he stayed in Human Robot Research Center in Korea Institute of Science and Technology as a senior researcher. He was a professor in the Division of Electronics and Information Engineering, Chonbuk National University, Korea from September 1999 to February 2007. He was also a post doctorial researcher in the Department of Computer Science, University of Southern California, Los Angeles in 1997 and a visiting researcher in the Dept. of Electrical and Computer Engineering, University of Illinois at Urbana-Champaign in 2005. He is now with the Department of Electrical and Information Engineering in Seoul National University of Science and Technology, Korea. His primary research interest is in the area of robot vision, and intelligent control theory.

Phan Bui Khoi received his Doctorate degree in Robotics from Mechanical Engineering Research Institute of the Russian Academy of Sciences in 1997. He is an Associate Professor of dynamics and control of robot and mechatronic system at Hanoi University of Science and Technology. His current research, which focuses on robots applying in mechanical engineering and service, is concerned with dynamics of serial. Parallel and cooperate robots, force control, fuzzy control; control of robots and mechatronic systems based on artificial intelligence, hedge algebras, and genetic algorithm.

References

[1] ISO 10218-1:2011. Robot for industrial environments – safety requirements – part 1: robot, technical report. Geneva, Switzerland: International Organization for Standardization; 2011.

[2] Navarro B, Cherubini A, Fonte A, et al. An ISO10218-compliant adaptive damping controller for safe physical human-robot interaction. 2016 IEEE International Conference on Robotics and Automation (ICRA); Stockholm, Sweden; 2016. p. 3043–3048.

[3] Jindai M, Watanabe T. A handshake robot system based on a shake-motion leading model. 2008 IEEE/RSJ International Conference on Intelligent Robots and Systems (IROS); Nice, France; 2008. p. 3330–3335.

[4] Kovács S, Vincze D, Gacsi M, et al. Fuzzy automaton based human-robot interaction. SAMI 2010 8th IEE International Symposium on Applied Machine Intelligence and Informatics; Herlany, Slovakia; 2010. p. 165–169.

[5] Kovács S, Vincze D, Gacsi M, et al. Interpolation based fuzzy automaton for human-robot interaction. 9th IFAC Symposium on Robot Control. 2009;42(16):317–322.

[6] Papageorgiou D, Doulgeri Z. A Kinematic controller for human-robot handshaking using internal motion adaption. 2015 IEEE International Conference on Robotics and Automation; WA, USA; 2015. p. 5622–5627.

[7] Dimeas F, Mouolianitis V, Papakonstantinou C, et al. Manipulator performance constraints in Cartesian admittance control for human-robot cooperation. 2016 IEEE International Conference on Robotics and Automation (ICRA); Stockholm, Sweden; 2016. p. 3049–3054.

[8] Takagi T, Sugeno M. Fuzzy identification of systems and its applications to modeling and control. IEEE Trans Syst Man Cybern. 1985;SMC-15(1):116–132.

[9] Mamdani E. Twenty years of fuzzy control: experiences gained and lessons learnt. IEEE International Conference on Fuzzy Systems; San Francisco, CA, USA; 1993. p. 339–344.

[10] Wang L. Stable adaptive fuzzy control of nonlinear systems. IEEE Trans Fuzzy Syst. 1993;1(2):146–155.

[11] Wang L. A course in fuzzy systems and control. Upper Saddle River (NJ): Prentice-Hall; 1997.

[12] Su C, Stepanenko Y. Adaptive control of a class of nonlinear systems with fuzzy logic. IEEE Trans Fuzzy Syst. 1994;2(4):285–294.

[13] Yang YS, Jia XL, Zhou CJ. Robust adaptive fuzzy control for a class of uncertain nonlinear systems. 4th International Conference of Intelligent Techniques Soft Computing Nuclear Science Engineering; Bruges, Belgium; 2000. p. 303–311.

[14] Dimeas F, Aspragathos N. Fuzzy learning variable admittance control for human-robot cooperation. 2014 IEEE/RSJ International Conference on Intelligent Robots and Systems; Chicago (IL), USA; 2014. p. 4770–4775.

[15] Jamil M, Jalani J, Ahmad A. A new approach of active compliance control via fuzzy logic control for multifingered robot hand. First International Conference on Intelligent Robots and Systems; 2014. p. 4770–4775.

[16] Khoi P, Toan N. Application of fuzzy logic for controlling mechanism of relative manipulation robot (MRM robot). J Sci Technol. 2016;54(3):385–401.

[17] Toan N, Khoi P. A control solution for closed-form mechanisms of relative manipulation based on fuzzy approach. Int J Adv Rob Syst. 2019;16(2):1–11.

[18] Toan N, Kim J, Kim K, et al. Application of fuzzy logic to damping controller for safe human-robot interaction. 14th International Conference on Ubiquitous Robots and Ambient intelligence; Jeju, South Korea; 2017. p. 109–113.

[19] Toan N, Khoi P. Fuzzy-based admittance controller for safe natural human-robot interaction. Adv Robot. 2019;33(15-16):815–823.

[20] Ho N, Wechler W. Hedge algebras: An algebraic approach to structure of sets of linguistic truth values. Fuzzy Sets Syst. 1990;35(3):281–293.

[21] Ho N, Wechler W. Extended hedge algebras and their application to fuzzy logic. Fuzzy Sets Syst. 1992;52(3):259–281.

[22] Ho N, Nam H. An algebraic approach to linguistic hedges in Zadeh's fuzzy logic. Fuzzy Sets Syst. 2002;129(2):229–254.
[23] Ho N, Tran T, Pham D. Modeling of a semantics core of linguistic terms based on an extension of hedge algebra semantics and its application. Knowl Based Syst. 2014;67:244–262.
[24] Khoi P, Toan N. Hedge-algebras-based controller for mechanisms of relative manipulation. Int J Prec Eng Manuf. 2018;19(3):377–385.
[25] Phong P, Dong D, Khang T. Hedge algebra based type-2 fuzzy logic system and its application to predict survival time of myeloma patients. International Conference on Knowledge and Systems Engineering; 2009. p. 13–18.
[26] Bui H, Tran D, Vu N. Optimal fuzzy control of an inverted pendulum. J Vib Control. 2012;18(14):2097–2110.
[27] Bui H, Nguyen C, Bui V, et al. Vibration control of uncertain structures with actuator saturation using hedge-algebras-based fuzzy controller. J Vib Control. 2015;23(12):1–19.
[28] Duc N, Vu N, Tran D, et al. A study on the application of hedge algebras to active fuzzy control of a seism-excited structure. J Vib Control. 2012;18(14):2186–2200.
[29] Nguyen C, Pedrycz W, Duong T, et al. A genetic design of linguistic terms for fuzzy rule based classifiers. Int J Approx Reason. 2013;54(1):1–21.
[30] Vukadinović D, Bašić M, Nguyen C, et al. Hedge-algebra-based voltage controller for a self-excited induction generator. Control Eng Pract. 2014;30:78–90.
[31] Ali O, Ali A, Sumait B. Comparison between the effects of different types of membership functions on fuzzy logic controller performance. Int J Emerging Eng Res Technol. 2015;3(3):76–83.
[32] Naaz S, Alam A, Biswas R. Effect of different defuzzification methods in a fuzzy based load balancing application. Int J Comput Sci Issues. 2011;8(1):261–267.
[33] Buss S. 3D computer graphics: A mathematical introduction with OpenGL. New York (NY): Cambridge University Press; 2003.
[34] Tsumugiwa T, Yokogawa R, Yoshida K. Stability analysis for impedance control of robot for human-robot cooperative task system. 2004 IEEE/RSJ International Conference on Intelligent Robots and Systems; Sendai, Japan; 2004. p. 3883–3888.
[35] Mussa-Ivaldi F, Hogan N, Bizzi E. Neural, mechanical, and geometric factors subserving arm posture in humans. J Neurosci. 1985;5(10):2732–2743.
[36] Phan KB, Ha HT, Hoang SV. Eliminating the effect of uncertainties of cutting forces by fuzzy controller for robots in millings process. Appl Sci. 2020;10(5):1685.
[37] Cat HN, Nhu LV, Le Xuan V. An Interpolative reasoning method based on hedge algebras and its application to a problem of fuzzy control. Proceedings of the 10th WSEAS International Conference on Computers, Vouliagmeni; Athens, Greece, July 13–15, 2006, pp. 526–534.
[38] Ho NC, Lan VN, Viet LX. Optimal hedge-algebras-based controller: Design and application. Fuzzy Sets Syst. 2008;159:968–989.